Elastic Buckling of Orthotropic Plates under Varying Axial Stresses

A. BADIR, H. HU AND A. DIALLO

IN-39

061 129

P. 10

ABSTRACT

The elastic buckling load of simply supported rectangular orthotropic plates subjected to a second degree parabolic variation of axial stresses in the longitudinal direction is calculated using analytical methods. The variation of axial stresses is equilibrated by nonuniform shear stresses along the plate edges and transverse normal stresses. The influence of the aspect ratio is examined, and the results are compared with plates subjected to uniform axial stresses.

INTRODUCTION

In most studies of stability of plates, the axial stress has been taken as uniform compression throughout flat rectangular plates (Timoshenko and Gere, 1961; Allen and Bulson, 1980; Whitney, 1987). Buckling of isotropic plates under a compressive stress that varies linearly from one loaded edge to the other has been studied by Libove, Ferdman and Reusch (1949). Cases of practical interest exist, however, in which the axial stress is not uniform but varies from tension at both loaded edges to compression in the middle. An example is the stability of the crown of the hat stiffened panel, a candidate configuration of the upper and lower skin of the Blended Wing Body (BWB) Aircraft. The BWB Aircraft is an advanced long-range ultra-high-capacity airliner with the principal feature being the wide double-deck body which is blended into the wing (Popular Science Magazine, 1995).

In the present paper, analytical methods are used to investigate the local stability of the hat crown plate in order to minimize its weight while optimizing its buckling strength. A varying tension-compression-tension stress is induced in the crown of the stiffeners. The axial stresses vary longitudinally due to bending, and the change in stresses is equilibrated by nonuniform shear stresses along the plate edges and transverse normal stresses as shown in Fig. 1.

ANALYTICAL MODEL

The distribution of the axial stresses is given by

Ashraf Badir, Assistant Professor, Department of Engineering, Clark Atlanta University, Atlanta, GA 30314

Hurang Hu, Research Associate, Department of Engineering, Clark Atlanta University, Atlanta, GA 30314

Abdouramane Diallo, Graduate Student, Department of Mathematics, Clark Atlanta University, Atlanta, GA 30314

$$\sigma_x(x) = \left[1 - 6\left(\frac{x}{a}\right) + 6\left(\frac{x}{a}\right)^2\right]\sigma_x\big|_{x=0} \tag{1}$$

and the expressions for the shear and transverse normal stresses $\tau_{xy}(x,y)$ and $\sigma_y(y)$, are obtained by integrating the plane stress equilibrium equations

$$\frac{\partial \sigma_x}{\partial x} + \frac{\partial \tau_{xy}}{\partial y} = 0 \tag{2}$$

$$\frac{\partial \sigma_y}{\partial y} + \frac{\partial \tau_{xy}}{\partial x} = 0 \tag{3}$$

and are found to be

$$\tau_{xy}(x,y) = -3\frac{b}{a}(1 - \frac{2x}{a})(1 - \frac{2y}{b})\sigma_x\big|_{x=0} \tag{4}$$

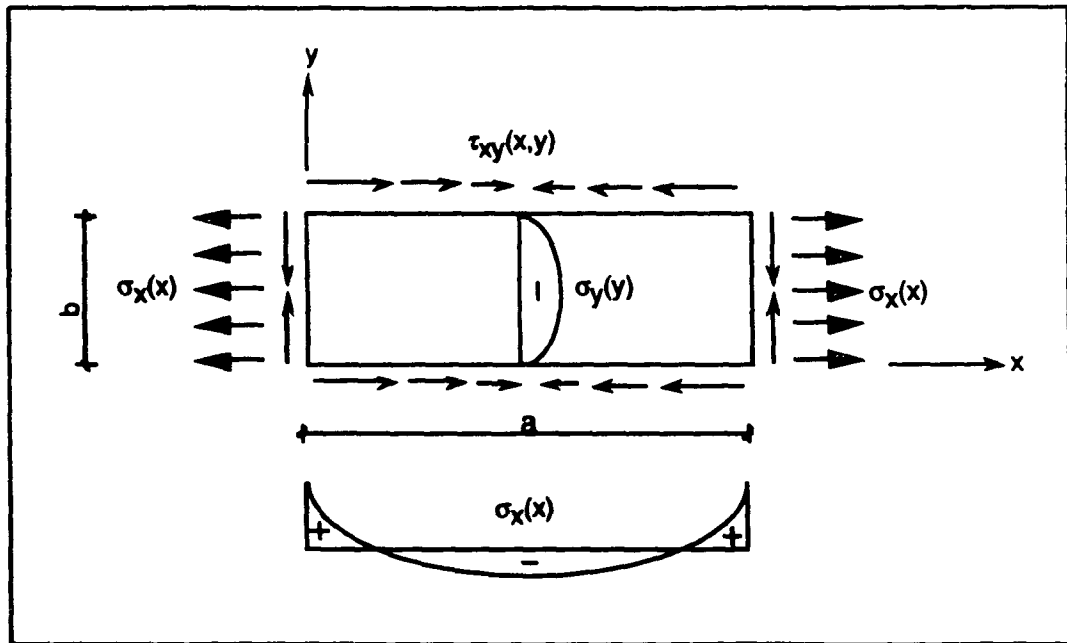$$\sigma_y(y) = 6\left(\frac{b}{a}\right)^2 \frac{y}{b}\left(\frac{y}{b} - 1\right)\sigma_x\big|_{x=0} \tag{5}$$

Figure 1. Plate subjected to tensile/compression/tensile longitudinal stresses $\sigma_{xx}(x)$, equilibrated by shear stresses $\tau_{xy}(x,y)$ and transverse stresses $\sigma_{yy}(y)$

The differential equation of the deflection surface of the orthotropic plate can be written as follows:

$$D_{11}\frac{\partial^4 w}{\partial x^4} + 2(D_{12} + 2D_{66})\frac{\partial^4 w}{\partial x^2 \partial y^2} + D_{22}\frac{\partial^4 w}{\partial y^4} - N_x\frac{\partial^2 w}{\partial x^2} - 2N_{xy}\frac{\partial^2 w}{\partial x \partial y} - N_y\frac{\partial^2 w}{\partial y^2} = 0 \tag{6}$$

where D_{ij}, w, N_x, N_{xy}, and N_y are the bending stiffnesses of the orthotropic plate (Jones, 1975), vertical displacement, axial, shear and transverse stress resultants, respectively. A solution to Eq. (6) that satisfies the boundary conditions cannot be obtained in closed form. Thus, approximate solutions are sought. Two different displacement fields are considered· (1) Double Fourier series, using Rayleigh-Ritz method, and (2) a polynomial in the longitudinal direction, using Galerkin method. A summary of the analytical models is described in the next sections, the influence of the aspect ratio is examined, and the results are compared with plates subjected to uniform axial loads.

DOUBLE FOURIER SERIES (RAYLEIGH-RITZ METHOD)

The total potential energy functional of the orthotropic plate is given by

$$U = \frac{1}{2}\int_0^a\int_0^b \left\{ D_{11}\left(\frac{\partial^2 w}{\partial x^2}\right)^2 + 2D_{12}\frac{\partial^2 w}{\partial x^2}\frac{\partial^2 w}{\partial y^2} + D_{22}\left(\frac{\partial^2 w}{\partial y^2}\right)^2 + 4D_{66}\left(\frac{\partial^2 w}{\partial x \partial y}\right)^2 + \sigma_x t\left(\frac{\partial w}{\partial x}\right)^2 \right.$$

$$\left. + \sigma_y t\left(\frac{\partial w}{\partial y}\right)^2 + 2\tau_{xy} t\frac{\partial w}{\partial x}\frac{\partial w}{\partial y} \right\} dy\, dx \tag{7}$$

where t, a, and b represent the thickness, length and width of the plate, respectively.

Of all conceivable buckling patterns satisfying boundary conditions, the actual buckling pattern is that for which the potential energy U, as given by Eq. (7), is a minimum. The deflection surface of the simply supported skin in bending may be represented by a Double Fourier series as

$$w = \sum_{m=1}^{M}\sum_{n=1}^{N} a_{mn}\sin\frac{m\pi x}{a}\sin\frac{n\pi y}{b} \tag{8}$$

which satisfies the simply supported boundary conditions. Rayleigh-Ritz method requires that the coefficients a_{mn} be chosen such that U is a minimum. That is, they must satisfy the equations

$$\frac{\partial U}{\partial a_{ij}} = 0 \quad (i = 1,2...M; \quad j = 1,2...N) \tag{9}$$

The deflection expression (8) can be splitted into two independent subsets, one corresponding to even values of n and the other, to odd values of n. The first subset corresponds to buckling that is antisymmetric about the line $y = b/2$ and the second, to buckling that is symmetric about that line. The second subset gives lower buckling loads, and attention is hereinafter confined to it. Similar argument can be made to the buckling pattern in the longitudinal direction (subscript m). Therefore, the buckling pattern is chosen as

$$w = \sum_{m=1,3,5}^{M} \sum_{n=1,3,5..}^{N} a_{mn} \sin\frac{m\pi x}{a} \sin\frac{n\pi y}{b}$$

(10)

Substituting Eqs. (1), (4-5), and (10) into the energy expression (7), while using Eq. (9), we obtain the following relations

$$A_{mn}a_{mn} + \sum_{i=1,3,5...}^{M} B_i a_{in} + \sum_{j=1,3,5...}^{N} C_j a_{mj} + \sum_{i=1,3,5...}^{M} \sum_{j=1,3,5...}^{N} D_{ijmn}a_{ij} = 0 \qquad \begin{cases} m = 1,3,5...M \\ n = 1,3,5...N \end{cases}$$

(11)

where

$$A_{mn} = \frac{D_{11}\pi^2}{N_0 b^2}(\frac{m^4}{\beta^2} + \frac{2(D_{12}+2D_{66})}{D_{11}}m^2 n^2 + \frac{D_{22}}{D_{11}}n^4\beta^2) + m^2$$

$$\beta_i = mi \begin{cases} -1, & m = i \\ \dfrac{12}{\pi^2}\left[\dfrac{1}{(m+i)^2} + \dfrac{1}{(m-i)^2}\right], & |m \pm i| = even \end{cases}$$

$$C_j = nj \begin{cases} -1, & n = j \\ \dfrac{12}{\pi^2}\left[\dfrac{1}{(n+j)^2} + \dfrac{1}{(n-j)^2}\right], & |n \pm j| = even \end{cases}$$

$$D_{ijmn} = \frac{1}{\pi^2} \begin{cases} -6, & m = i, n = j \\ \dfrac{96mnij}{\left(m^2 - i^2\right)\left(n^2 - j^2\right)}, & m \neq i, n \neq j, |m \pm i| = even, |n \pm j| = even \end{cases}$$

and

$$\beta = \frac{a}{b} \qquad \text{and} \qquad N_0 = t\sigma_x\big|_{x=0}$$

(12)

β and N_0 represent the aspect ratio and buckling load, respectively. A nondimensional buckling coefficient k may be expressed as

$$k = \frac{N_0 b^2}{D_{11} \pi^2} \tag{13}$$

Relations (11) represent a set of $(M+1)(N+1)/4$ linear equations. the smallest eigenvalue of Eqs. (11) gives the buckling load.

POLYNOMIAL (GALERKIN METHOD)

We seek a nontrivial solution to the deflection w which satisfies equation (6) and the boundary conditions. For simply supported plates, the solution of Eq. (6) may be represented by

$$w = \sum_{m=1}^{M} \sum_{n=1}^{N} q_{mn} \left(\xi^{m+3} + A_{m1} \xi^{m+2} + A_{m2} \xi^{m+1} + A_{m3} \xi^m + A_{m4} \xi^{m-1} \right) \sin(n\pi\eta) \tag{14}$$

in which $\xi = x/a$; $\eta = y/b$ and the coefficients $A_{m1} \sim A_{m4}$ are determined by satisfying the four simply supported boundary conditions at the two loaded sides.

The expression for the Galerkin equations is given by

$$\int_{\eta=0}^{1} \int_{\xi=0}^{1} \left\{ D_{11} \left(\frac{\partial^2 w}{\partial x^2} \right)^2 + 2D_{12} \frac{\partial^2 w}{\partial x^2} \frac{\partial^2 w}{\partial y^2} + D_{22} \left(\frac{\partial^2 w}{\partial y^2} \right)^2 + 4D_{66} \left(\frac{\partial^2 w}{\partial x \partial y} \right)^2 \right.$$

$$\left. + \sigma_x t \left(\frac{\partial^2 w}{\partial x^2} \right)^2 + \sigma_y t \left(\frac{\partial^2 w}{\partial y^2} \right)^2 + 2\tau_{xy} t \frac{\partial w}{\partial x} \frac{\partial w}{\partial y} \right\} \frac{\partial w}{\partial q_{mn}} d\xi \, d\eta = 0 \qquad (m = 1,2\ldots M; n = 1,2\ldots N) \tag{15}$$

Theses relationships represent a set of $M \times N$ homogeneous algebraic equations. In order to avoid a trivial solution $(q_{mn} = 0)$, the nondimensional buckling load k is chosen such that the determinant of the coefficient matrix vanishes. The minimum value of k that satisfies the requirement is the buckling load.

TABLE I. MATERIAL PROPERTIES

E_{11}	E_{22}	G_{12}	υ_{12}
9.25 Msi	4.67 Msi	2.27 Msi	0.397

TABLE II. CONVERGENCE OF BUCKLING COEFFICIENT k FOR A SQUARE PLATE

M/N	1	3	5	7
1	1.75	1.69	1.65	1.65
3	1.72	1.65	1.65	1.65
5	1.72	1.65	1.65	
7	1.72	1.65		
9	1.72			

RESULTS

First, a convergence study for Rayleigh-Ritz method is performed. Orthotropic plates with material properties as listed in Table I have been studied. For a square plate, buckling coefficients k versus increasing values of M and N are listed in Table II. It can be seen that when $M=N=3$, k reaches its final value. Convergence of the solution in this case is faster than in the case of long strips. For example a four-term series ($M = N = 3$, note that only odd M and N are considered) converges to the final k value compared to a 12-term solution ($M = 23$, $N = 1$) for a long strip with $\beta = 20$.

The buckling coefficient k versus aspect ratio β is plotted in Fig. 2. Figure 2 shows that for plates with aspect ratio less than six, the buckling coefficient k increases as β increases. However, for long strips ($\beta > 6$), k does not significantly change and takes a value of approximately 5.75.
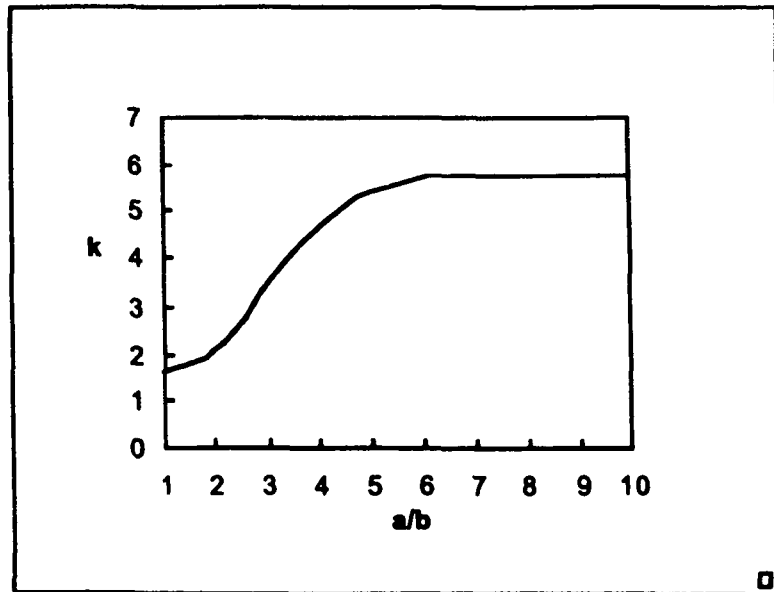

Figure 2. Buckling coefficient versus aspect ratio

TABLE III. CONVERGENCE OF BUCKLING COEFFICIENT FOR A SQUARE PLATE USING GALERKIN METHOD.

M	k
1	2.54
2	1.96
3	1.79
4	1.68
5	1.66

Galerkin method is also used to calculated the buckling load. The accuracy of the polynomial representation of the displacement field in the longitudinal direction, given by Eq (14), is examined for a square plate. The values of the buckling coefficient k are listed in Table III, converging to a value of 1.66 ($M=5$, $N=1$) compared to 1.65 as obtained using Fourier Series (Rayleigh-Ritz method, Table II). For $M=5$ and $N=1$, the displacement w, Eq. (14) takes the following form

$$w = \left[q_{11}\left(\xi^4 - 2\xi^3 + \xi\right) + q_{21}\left(3\xi^5 - 10\xi^3 + 7\xi\right) + q_{31}\left(7\xi^6 - 12\xi^5 + 5\xi^3\right)\right.$$
$$\left. + q_{41}\left(\xi^7 - 6\xi^4 + 5\xi^3\right) + q_{5m}\left(4\xi^8 - 22\xi^5 + 18\xi^4\right)\right]\sin(\pi\eta) \qquad (16)$$

The buckling load intensity (load per unit width) calculated based on a parabolic and uniform load distribution is listed in Table IV. The parabolic load values represent the buckling load intensity at mid-span of the plate (i.e., $t\sigma_x\big|_{x=a/2}$ or $kD_{11}\pi^2/2b^2$).

Table IV shows that the buckling load intensity is influenced by both the load distribution and the aspect ratio. For a square plate, the buckling load calculated based on a uniform stress distribution is 244% higher than the buckling load calculated based on a tensile/compressive/tensile parabolic load distribution. The difference is only 5% (reduction)

TABLE IV. COMPARISON OF BUCKLING COEFFICIENTS FOR VARYING AXIAL STRESS AND UNIFORM STRESS

	Parabolic Load* (lb/in)		Uniform Load[¹] (lb/in)	% diff.
	Fourier Series	Polyno-mial	Exact	
a=b=150 in (a/b=1)	1.35[†]	1.36[†]	4.64	+244%
a=150 in. b=4.3 in. (a/b=35)	5773[†]	...	5482	-5%

* Associated with shear and transverse stresses as given in Eqs. (4) and (5).
[¹] No shear and transverse stresses.
[†] Buckling Load intensity at mid-span (x=a/2).

for long strips. One may expect that a tensile stress at the edges as shown in Fig. 1 will tend to restore the plate to its stable position and therefore increases its buckling load. However, the parabolic stress distribution is associated with both compressive and shear stresses   The transverses compressive stresses $\sigma_y(y)$ have a detrimental effect on the buckling load for square plates, while their effect is negligible for long strips.

CONCLUSIONS

The elastic buckling load of orthotropic plates subjected to a parabolically varying tension-compression-tension longitudinal stress, equilibrated by nonuniform shear stresses and transverse compressive stresses is analyzed. It is shown that the buckling load depends on the aspect ratio for plates with aspect ratio less than six. For square plates, the buckling load due to a uniform stress distribution is 244% higher than the buckling load calculated based on a tensile/compressive/tensile parabolic load distribution. However, the difference is only 5% (reduction) for long strips.

ACKNOWLEDGMENT

REFERENCES

Allen, H. G., and P S Bulson, 1980. "Background to Buckling," McGraw-Hill Book Company

Jones, R. M. 1975. "Mechanics of Composite Materials," McGraw-Hill, New York

Libove, C., S. Ferdman, and J. Reusch. 1949. "NACA Tech. Note No. 1891."

Popular Science Magazine, April, 1995

Timoshenko, S P and J. M. Gere, 1961. "Theory of Elastic Stability," 2nd ed   McGraw-Hill Book Company.

Whitney, J M. 1987. "Structural Analysis of Laminated Anisotropic Plates," Technomic Publishing Company.